

# Tree-level irrigation inference using UAV thermal imagery and convolutional neural networks

Haoyu Niu<sup>1</sup>, Dong Wang<sup>2</sup>, and YangQuan Chen<sup>3</sup>

**Abstract**—Irrigation management has been one of the keys to achieve sustainability and marketability in agriculture, which is estimated to account for over 70% of global water use. The optimal use of water through irrigation is important for the evolution of agriculture. Many progressive growers make irrigation decisions using crop evapotranspiration (ETc). With the advent of Unmanned Aerial Vehicles (UAVs), lightweight sensors, such as thermal camera, can be mounted on the UAVs to take high-resolution images. Compared with satellite imagery, the spatial resolution of the UAV images can be at the centimeter level. Thus, in this article, the authors proposed a reliable individual tree-level irrigation inference system using a small UAV platform and Convolutional Neural Networks (CNNs). A field study was conducted at the USDA-ARS Research Center in Parlier, California to train and test CNN models using images of the pomegranate trees. The pomegranate field was randomly designed into 16 equal blocks to test two irrigation levels, the low irrigation volume (35% and 50% of ETc) and high irrigation volume (75% and 100% of ETc), measured by a weighing lysimeter in the field. Results showed that the trained CNN model could successfully classify the individual tree using the thermal UAV imagery into the targeted irrigation levels. The overall prediction accuracy was around 87%, which showed a state-of-art performance and indicated that UAV thermal imagery could infer the irrigation levels at individual tree level.

## I. INTRODUCTION

The tree canopy temperature from infrared thermometer (IRT) sensors is an effective tool for detecting plant water stress. Research has been conducted on crops and trees to relate the midday infrared canopy to air temperature difference ( $\Delta T$ ) to irrigation management. The main reason is that a significant increase in  $\Delta T$  will indicate stomata closure and water stress conditions [1], [2], [3]. For example, Zhang and Wang evaluated the performance of using  $\Delta T$  to manage postharvest deficit irrigation of nectarine trees in [4]. The results demonstrated that the measured  $\Delta T$  values above the tree canopy showed consistent differences among irrigation treatment levels. Clawson and Blad used canopy temperature variability and average canopy temperature to schedule irrigation in corn (*Zea mays* L.). They remarked that canopy temperature variability could show the plant water stress and the need to schedule an irrigation event [5]. Furthermore, Wang and Gartung investigated the infrared canopy temperature of early ripening peach trees under postharvest

deficit irrigation and monitored the stem water potential [6]. The strong correlation between stem water potential and  $\Delta T$  ( $R^2 \approx 0.7$ ) indicated that canopy temperature could be used for water status estimation.

However, little research could be found in the literature on using midday  $\Delta T$  derived from UAV thermal infrared (TIR) image as a primary input for mapping irrigation treatment levels of a pomegranate field at individual tree level. This article evaluated the feasibility and performance of using midday  $\Delta T$  (UAV-TIR) and CNN algorithms for tree water status inference. Recently, UAV has been emerging as a powerful platform in agricultural applications, such as irrigation management [7], [8], [9], and water stress estimation [10], [11], [12], [13]. With lightweight sensors being mounted on UAVs, high spatial and temporal resolution imagery has been taken in massive amounts with low cost [14], [15], [16]. Because of the lightweight and low power consumption characteristics, the thermal camera has been commonly used in agriculture research [17], [18].

Convolutional neural network (CNN) is one of the most common architectures, which includes the input layer, the convolution layer, the pooling layer and the fully connected layer [19]. Because of its powerful ability for complex data analysis, CNN models have been commonly used in agricultural applications, such as yield estimation [20], water stress analysis [21], and pest management [22]. For example, Yang *et al.* proposed to estimate corn yield by using the hyperspectral imagery and a CNN model in [23]. Research results showed that the spectral and color image-based integrated CNN model had a classification accuracy of 75.5%. In [22], Li *et al.* proposed an effective data augmentation strategy for CNN-based method for pest detection. In the training phase, they adopted data augmentation by rotating images with several degrees followed by cropping into different grids. Then, a large number of extra multi-scale examples were obtained and could be used to train a multi-scale pest detection model. Experimental results showed that their data augmentation strategy with CNN model achieved the pest detection accuracy of 81.4%. Advances in CNN models have been leading to significantly promising progress for agricultural research.

The **objectives of this article** were: 1. Evaluated the reliability of the UAV thermal camera on individual tree canopy temperature measurements. 2. Demonstrated the performance of the CNN model on irrigation treatment inference. The **major contributions of this article** were: 1. Developed a reliable tree-level water stress detection method using UAV-based high-resolution thermal images. 2. Proposed a CNN

<sup>1</sup>Haoyu Niu is a Ph.D. candidate at University of California, Merced, 5200 Lake Rd, Merced, CA 95340, USA hniu2@ucmerced.edu

<sup>2</sup>Dr. Dong Wang is a Lead Reseacher at USDA-ARS Water Management Research Unit, San Joaquin Valley Agricultural Sciences Center, Parlier, CA dong.wang@ars.usda.gov

<sup>3</sup>Prof. YangQuan Chen is a professor at University of California, Merced, 5200 Lake Rd, Merced, CA 95340, USA ychen53@ucmerced.edu



Fig. 1. The pomegranate field at the USDA-ARS (36.594°N, 119.512°W). The weighing lysimeter is located in the center of the pomegranate field, marked as a red box. The blue marks are where the 14 IRT sensors were installed.

model and proved its performance on the classification of tree-level water status. The rest of the paper was organized as follows. Section II introduced the materials and methods being used for UAV-based irrigation treatment inference. Results and discussion were presented in Section III. In Section IV, the authors drew the conclusive remarks.

## II. MATERIAL AND METHODS

### A. Study site and irrigation management

The study was conducted in a 1.3 ha pomegranate field in 2019 at the USDA-ARS San Joaquin Valley Agricultural Sciences Center in Parlier, CA (36.594°N, 119.512°W). The pomegranate (*Punica granatum* L., cv 'Wonderful') was planted in 2010 with a 5 m spacing between rows and a 2.75 m within-row tree spacing [24]. There are also two large weighing lysimeters, which are 2 m × 4 m by 3 m in depth and have a resolution of 0.1 mm of water loss. As shown in Fig. 1, the weighing lysimeters are located in the center of the pomegranate field. The experimental site was randomly designed into 16 blocks to test effects of irrigation rates on the pomegranate growth. As measured by the lysimeter, the irrigation volumes were set up as 35%, 50%, 75%, and 100% of crop ET or ET<sub>c</sub>. The trees in the lysimeter were irrigated at the 100% level. For each irrigation treatment block, there were three rows with 15 trees per row. Only the central row of each block was used as the experimental row.

### B. Ground truth: Infrared canopy and air temperature

The tree canopy temperature was measured with wireless infrared thermometers or IRTs (Dynamax Inc., Houston, TX), which were installed 4.5 m above the soil surface. The field of view (FOV) of the IRT sensor was 20° (Fig. 2). The air temperature and relative humidity were also measured with a sensor in the experimental site.

### C. Thermal infrared remote sensing data

1) *Description of the UAV and thermal camera:* A quadcopter named "Foxtech Hover" was used as the low-cost

UAV platform (less than \$1000) to collect high-resolution thermal images at the height of 60 m. The UAV was equipped with a highly efficient power system, including T-Motor MN3508 KV380 motors, 1552 folding propellers, and Foxtech Multi-Pal 40A OPTP ESC, to ensure long flight time. The UAV also included a Pixhawk flight controller, GPS, and telemetry antennas, enabling it to fly over the pomegranate field by waypoints mode (designed using Mission Planner software). The Hover's lithium-polymer battery had a capacity of 9500 mAh, which could support 30-minute flight missions with the thermal camera mounted on the UAV. The thermal camera ICI 9640 P (Infrared Cameras Inc, Beaumont, TX, USA.)<sup>1</sup> was used for collecting thermal images for the experimental field. The sensor has a resolution of 640 × 480 pixels. The spectral band is from 7 μm to 14 μm. The dimension of the thermal camera is 34 mm × 30 mm × 34 mm. The accuracy is designed to be ± 2 °C. A Raspberry Pi Model B computer (Raspberry Pi Foundation, Cambridge, UK.) was used to trigger the thermal camera during UAV flight missions.

2) *UAV thermal image collection and processing:* The authors used the Mission Planner to program all flight missions. The flight height was set up as 60 m. The overlapping of UAV imagery was set up as 80% so that the UAV imagery of the pomegranate could be stitched together more successfully during image processing. The UAV was flying at noon with clear sky conditions to minimize the shading effect on the thermal images. Since the thermal camera type was uncooled, it usually took around 20 minutes to warm up the thermal camera before flight missions. To calibrate the thermal camera, the authors took thermal images of ice water immediately before and after the flight missions as the reference temperature. After the flight missions, all

<sup>1</sup>Mention of trade names or commercial products in this publication is solely to provide specific information and does not imply recommendation or endorsement by the University of California or the U.S. Department of Agriculture. The University of California and the USDA are equal opportunity providers and employers.



Fig. 2. The IRT sensors were mounted on a cross arm attached to a metal pole 4.5 m above the soil surface, with a FOV of 20°. A quadcopter and a thermal camera were used to collect high-resolution thermal images at the height of 60 m.

TABLE I  
THE ARCHITECTURE OF THE CNN MODEL.

Layer Type	Output Shape	Parameter Numbers
Conv2D	(None, 30, 30, 32)	896
MaxPooling2D	(None, 15, 15, 32)	0
Conv2D	(None, 13, 13, 64)	18496
MaxPooling2D	(None, 6, 6, 64)	0
Conv2D	(None, 4, 4, 64)	36928
Flatten	(None, 1024)	0
Dense	(None, 64)	65600
Dense	(None, 2)	130

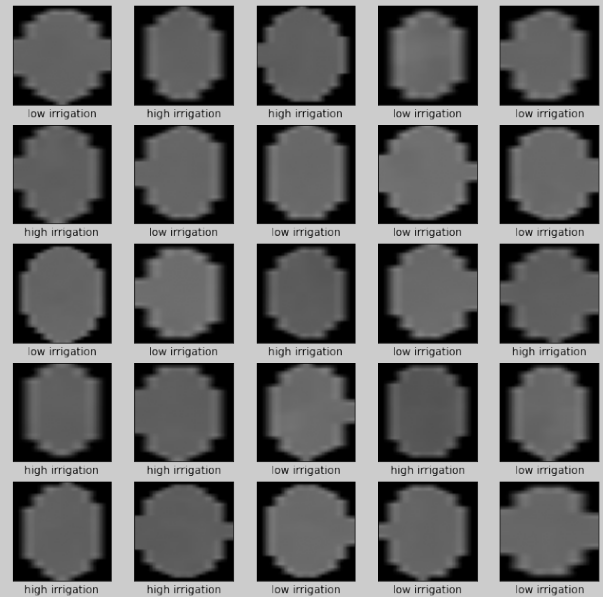


Fig. 3. 25 images were randomly selected from the training set and the class name for each image was displayed below. All the images were resized into  $32 \times 32 \times 3$  in order to input into the CNN model.

UAV thermal images were stitched together to generate the orthomosaick images in Metashape (Agisoft LLC, Russian).

3) *Image preprocessing for the CNN model:* The individual tree canopy images were extracted from the UAV thermal imagery, 250 in total. Then, the dataset was distributed as 67% for training and 33% for testing using the *train\_test\_split* method. To verify that the dataset looks correct, the authors plotted the first 25 images from the training set and displayed the class name below each image (Fig. 3). All the images were resized into  $32 \times 32 \times 3$  in order to input into our CNN model using TensorFlow 2.0. The summary of the CNN model is shown in Table I. The output of every Conv2D and MaxPooling2D layer is a 3D tensor of shape (height, width, channels). The width and height dimensions tend to shrink as we go deeper in the network. The number of output channels for each Conv2D layer is controlled by the first argument. The authors fed the last output tensor from the convolutional base into the Dense layers to perform classification. Dense layers take vectors as input (which are 1D), while the current output is a 3D tensor. Considering the dataset has two classes, the authors used a final Dense layer with 2 outputs.

### III. RESULTS AND DISCUSSION

#### A. Comparison of canopy temperature per tree based on ground truth and UAV thermal imagery

To evaluate the reliability of UAV thermal remote sensing, the authors first compared the canopy temperature per tree acquired by IRT sensors and the UAV thermal camera. The correlation between the canopy temperature per tree measured by the IRT sensors and UAV thermal camera was shown by their scatter-related plot and the established regression equation (Fig. 4). The coefficient of determination ( $R^2$ ) was 0.8668, which indicated that the difference between the ground truth and UAV thermal camera was acceptable. The UAV method was reliable for monitoring tree-level

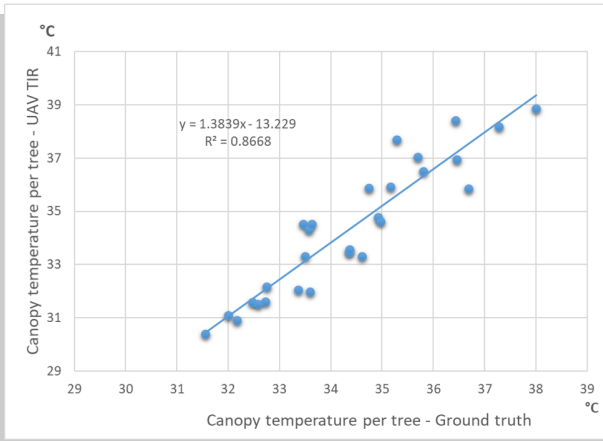


Fig. 4. The correlation between the canopy temperature per tree measured by the IRT sensors and UAV thermal camera. The coefficient of determination ( $R^2$ ) was 0.8668, which indicated that the difference between the ground truth and UAV thermal camera was acceptable. The method was reliable for monitoring tree-level canopy temperature.

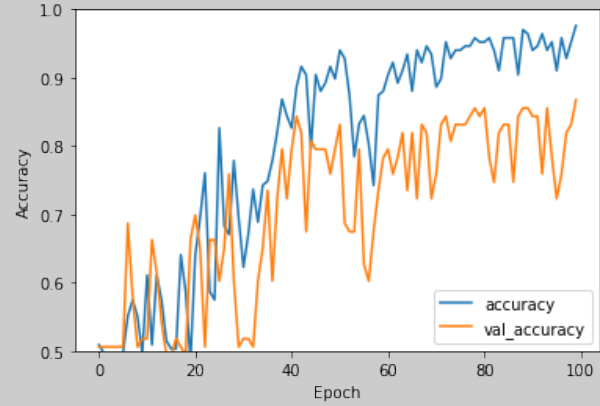


Fig. 5. The performance of the CNN model, training and validation accuracy curves.

canopy temperature.

### B. The performance of the CNN model

As mentioned earlier, there were 250 tree canopy images in total, which were distributed as 67% for training and 33% for testing using the *train\_test\_split* method. To train the CNN model, the ‘adam’ optimizer and the cross entropy loss function were adopted during the training process. The epoch was set up as 100. For evaluating the trained CNN models, the authors plotted the training and validation accuracy curves with the epochs increasing (Fig. 5). The test accuracy was 87%. To visualize the trained CNN model performance, the authors made predictions about some images in the test dataset (Fig. 7). Correct prediction labels are blue and incorrect prediction labels are red. The number gives the percentage (out of 100) for the predicted label. A confusion matrix was also used, which was a summary of prediction results on a classification problem. The number of correct and incorrect predictions was tallied with count values and divided into classes. The confusion matrix provided insight not only into the errors being made by a classifier but, more importantly, the types of errors that were being made. “True label” meant the ground truth of  $ET_c$  based irrigation treatment levels. “Predicted label” identified the irrigation treatment levels predicted by the trained CNN model. To simplify the visualization, low irrigation (30% and 50% ET) were labeled as “0”; high irrigation (75% and 100% ET) were labeled as “1” (Fig. 6). The detailed information of precision and recall was shown in Table II.

## IV. CONCLUSIONS

In this article, the authors collected the high-resolution thermal images by using a UAV-based lightweight payload. Irrigation treatment inference at the individual tree level was realized by using UAV-based thermal images and CNN model in a pomegranate field. The research results showed that the best classification accuracy of irrigation treatment

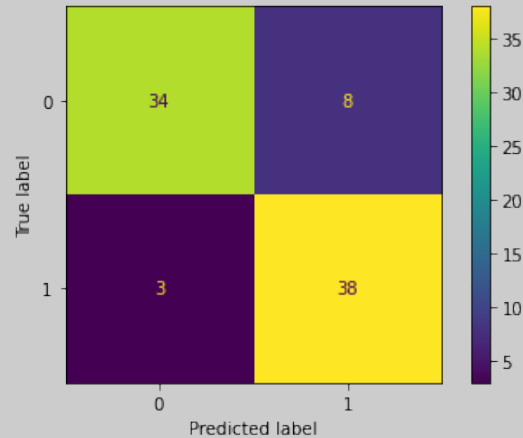


Fig. 6. The summary of prediction results on the irrigation treatment classification problem. “True label” meant the ground truth of  $ET_c$  based irrigation treatment levels. “Predicted label” identified the irrigation treatment levels predicted by the trained CNN model. To simplify the visualization, low irrigation (30% and 50% ET) were labeled as “0”; high irrigation (75% and 100% ET) were labeled as “1”.

TABLE II  
THE CNN MODEL PERFORMANCE.

Irrigation level	Precision	Recall	F1-score
Low irrigation	0.92	0.81	0.86
High irrigation	0.83	0.93	0.87
Accuracy	NA	NA	<b>0.87</b>
Macro avg	0.87	0.87	0.87
Weighted avg	0.87	0.87	0.87

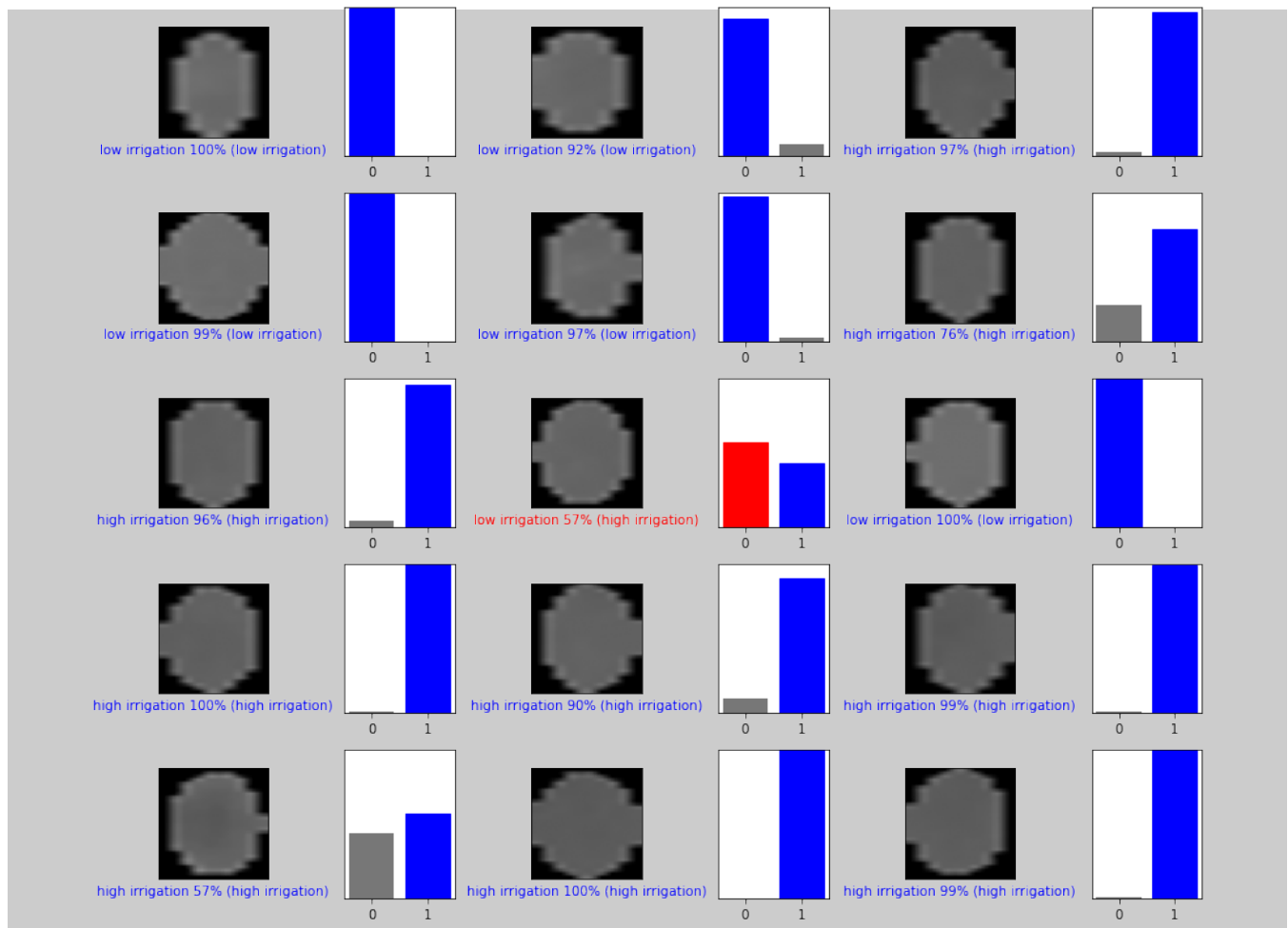


Fig. 7. To visualize the trained CNN model performance, the authors made predictions about some images in the test dataset. Correct prediction labels are blue and incorrect prediction labels are red. The number gives the percentage (out of 100) for the predicted label.

levels was 87% when the CNN model was adopted. The results of this research supported the idea that a significant increase in the midday infrared canopy to air temperature difference ( $\Delta T$ ) will indicate stomata closure and water stress conditions. The authors also proposed a CNN model and proved its performance on the classification of tree-level irrigation treatments. The research clearly demonstrated the capacity of new sensor technology and machine learning for making better-informed irrigation water management decisions. The authors developed a reliable tree-level irrigation treatment inference method using UAV-based high-resolution thermal images and CNN model.

#### ACKNOWLEDGMENT

Thanks go to Joshua Ahmed, Allan Murillo, Dong Sen Yan, Stella Zambruski and Christopher Currier for flying drones or collecting field measurements. We gratefully acknowledge the support of NVIDIA Corporation with the donation of the Titan X Pascal GPU used for this research.

#### REFERENCES

- [1] S. B. Idso, R. D. Jackson, and R. J. Reginato, "Remote-sensing of crop yields," *Science*, vol. 196, no. 4285, pp. 19–25, 1977.
- [2] R. D. Jackson, R. Reginato, and S. Idso, "Wheat canopy temperature: A practical tool for evaluating water requirements," *Water Resources Research*, vol. 13, no. 3, pp. 651–656, 1977.
- [3] R. D. Jackson, S. Idso, R. Reginato, and P. Pinter Jr, "Canopy temperature as a crop water stress indicator," *Water Resources Research*, vol. 17, no. 4, pp. 1133–1138, 1981.
- [4] H. Zhang and D. Wang, "Management of postharvest deficit irrigation of peach trees using infrared canopy temperature," *Vadose Zone Journal*, vol. 12, no. 3, pp. v2012-0093, 2013.
- [5] K. L. Clawson and B. L. Blad, "Infrared thermometry for scheduling irrigation of corn 1," *Agronomy Journal*, vol. 74, no. 2, pp. 311–316, 1982.
- [6] D. Wang and J. Gartung, "Infrared canopy temperature of early-ripening peach trees under postharvest deficit irrigation," *Agricultural Water Management*, vol. 97, no. 11, pp. 1787–1794, 2010.
- [7] T. Zhao, A. Koumis, H. Niu, D. Wang, and Y. Chen, "Onion irrigation treatment inference using a low-cost hyperspectral scanner," in *Multispectral, Hyperspectral, and Ultraspectral Remote Sensing Technology, Techniques and Applications VII*. International Society for Optics and Photonics, 2018.
- [8] H. Niu, T. Zhao, D. Wang, and Y. Chen, "A UAV resolution and waveband aware path planning for onion irrigation treatments inference," in *2019 International Conference on Unmanned Aircraft Systems (ICUAS)*. IEEE, 2019, pp. 808–812.

- [9] H. Niu, T. Zhao, J. Wei, D. Wang, and Y. Chen, "Reliable tree-level evapotranspiration estimation of pomegranate trees using lysimeter and UAV multispectral imagery," in *2021 IEEE Conference on Technologies for Sustainability (SusTech)*. IEEE, 2021, pp. 1–6.
- [10] T. Zhao, Y. Chen, A. Ray, and D. Doll, "Quantifying almond water stress using unmanned aerial vehicles (UAVs): Correlation of stem water potential and higher order moments of non-normalized canopy distribution," in *ASME 2017 International Design Engineering Technical Conferences and Computers and Information in Engineering Conference*. American Society of Mechanical Engineers, 2017.
- [11] V. Gonzalez-Dugo, P. Zarco-Tejada, E. Nicolás, P. A. Nortes, J. Alarcón, D. S. Intrigliolo, and E. Fereres, "Using high resolution UAV thermal imagery to assess the variability in the water status of five fruit tree species within a commercial orchard," *Precision Agriculture*, vol. 14, no. 6, pp. 660–678, 2013.
- [12] L. Santesteban, S. Di Gennaro, A. Herrero-Langreo, C. Miranda, J. Royo, and A. Matese, "High-resolution UAV-based thermal imaging to estimate the instantaneous and seasonal variability of plant water status within a vineyard," *Agricultural Water Management*, vol. 183, pp. 49–59, 2017.
- [13] J. Baluja, M. P. Diago, P. Balda, R. Zorer, F. Meggio, F. Morales, and J. Tardaguila, "Assessment of vineyard water status variability by thermal and multispectral imagery using an unmanned aerial vehicle (UAV)," *Irrigation Science*, vol. 30, no. 6, pp. 511–522, 2012.
- [14] T. Zhao, H. Niu, A. Anderson, Y. Chen, and J. Viers, "A detailed study on accuracy of uncooled thermal cameras by exploring the data collection workflow," in *Autonomous Air and Ground Sensing Systems for Agricultural Optimization and Phenotyping III*. International Society for Optics and Photonics, 2018.
- [15] S. Khanal, J. Fulton, and S. Shearer, "An overview of current and potential applications of thermal remote sensing in precision agriculture," *Computers and Electronics in Agriculture*, vol. 139, pp. 22–32, 2017.
- [16] H. Niu, D. Hollenbeck, T. Zhao, D. Wang, and Y. Chen, "Evapotranspiration estimation with small UAVs in precision agriculture," *Sensors*, vol. 20, no. 22, p. 6427, 2020.
- [17] K. Ribeiro-Gomes, D. Hernández-López, J. F. Ortega, R. Ballesteros, T. Poblete, and M. A. Moreno, "Uncooled thermal camera calibration and optimization of the photogrammetry process for UAV applications in agriculture," *Sensors*, vol. 17, no. 10, p. 2173, 2017.
- [18] H. Hoffmann, H. Nieto, R. Jensen, R. Guzinski, P. Zarco-Tejada, and T. Friborg, "Estimating evaporation with thermal UAV data and two-source energy balance models," *Hydrology and Earth System Sciences*, vol. 20, no. 2, pp. 697–713, 2016.
- [19] Y. LeCun, Y. Bengio, and G. Hinton, "Deep learning," *Nature*, vol. 521, no. 7553, pp. 436–444, 2015.
- [20] S. Khaki, L. Wang, and S. V. Archontoulis, "A CNN-RNN framework for crop yield prediction," *Frontiers in Plant Science*, vol. 10, p. 1750, 2020.
- [21] N. S. Chandel, S. K. Chakraborty, Y. A. Rajwade, K. Dubey, M. K. Tiwari, and D. Jat, "Identifying crop water stress using deep learning models," *Neural Computing and Applications*, vol. 33, no. 10, pp. 5353–5367, 2021.
- [22] R. Li, R. Wang, J. Zhang, C. Xie, L. Liu, F. Wang, H. Chen, T. Chen, H. Hu, X. Jia, *et al.*, "An effective data augmentation strategy for CNN-based pest localization and recognition in the field," *IEEE Access*, vol. 7, pp. 160 274–160 283, 2019.
- [23] W. Yang, T. Nigon, Z. Hao, G. D. Paiao, F. G. Fernández, D. Mulla, and C. Yang, "Estimation of corn yield based on hyperspectral imagery and convolutional neural network," *Computers and Electronics in Agriculture*, vol. 184, p. 106092, 2021.
- [24] H. Zhang, D. Wang, J. E. Ayars, and C. J. Phene, "Biophysical response of young pomegranate trees to surface and sub-surface drip irrigation and deficit irrigation," *Irrigation Science*, vol. 35, no. 5, pp. 425–435, 2017.